Biochimica et Biophysica Acta 1848 (2015) 654–661

Contents lists available at ScienceDirect

Biochimica et Biophysica Acta

journal homepage: www.elsevier.com/locate/bbamem

Transport across the outer membrane porin of mycolic acid containing actinomycetales: *Nocardia farcinica*

Pratik Raj Singh, Harsha Bajaj, Roland Benz, Mathias Winterhalter, Kozhinjampara R. Mahendran *

School of Engineering and Science, Jacobs University Bremen, Campus Ring 1, D-28759 Bremen, Germany

ARTICLE INFO

Article history:
Received 12 August 2014
Received in revised form 11 November 2014
Accepted 17 November 2014
Available online 23 November 2014

Keywords:
Nocardia farcinica
Antibiotic resistance
Mycolata
Porin
Single channel electrophysiology

ABSTRACT

The role of the outer-membrane channel from a mycolic acid containing Gram-positive bacteria *Nocardia farcinica*, which forms a hydrophilic pathway across the cell wall, was characterized. Single channel electrophysiology measurements and liposome swelling assays revealed the permeation of hydrophilic solutes including sugars, amino acids and antibiotics. The cation selective *N. farcinica* channel exhibited strong interaction with the positively charged antibiotics; amikacin and kanamycin, and surprisingly also with the negatively charged ertapenem. Voltage dependent kinetics of amikacin and kanamycin interactions were studied to distinguish binding from translocation. Moreover, the importance of charged residues inside the channel was investigated using mutational studies that revealed rate limiting interactions during the permeation.

1. Introduction

With the increasing awareness of antibiotic resistance against bacteria, recent findings have revealed a strong correlation of resistance with permeability changes of the cell wall [1–3]. The outer membrane of Gram-negative bacteria contributes to the intrinsic resistance by decreasing the flow of antimicrobial agents into the cell [4–6]. In contrast, Gram-positive bacteria lacking an outer membrane in their cell wall are in general, more sensitive to antibiotics [7]. A further group of Gram-positive bacteria belonging to the actinomycetales taxon, also called mycolata, has a high intrinsic resistance to a wide range of antibiotics due to the presence of an additional mycolic acid layer [7–10]. The mycolic acid layer is mainly composed of long chain mycolic acids and free lipids. It resembles the function of an outer membrane of Gram-negative bacteria [11–13].

Surprisingly, the cell envelope of mycolata also contains water-filled protein channels called porins, which facilitate the diffusion of hydrophilic molecules into the cell [14]. Porins spanning the outer membrane have been identified in the cell wall of some members of the mycolata, such as *Mycobacterium chelonea* [14,15], *Corynebacterium glutamicum* [16], *Mycobacterium smegmatis* [17] and *Nocardia farcinica* [18]. For example MspA, a porin from *M. smegmatis*, forms pores which allow the uptake of various sugars and hydrophilic antibiotics [19,20]. In recent years the importance of the role of porins in the uptake of antibiotics has been recognized in Gram-negative bacteria [21]. Additionally, Gram-positive mycolata group of bacterium comprises microorganisms such as *Mycobacterium tuberculosis* (TBC), *Mycobacterium leprae* (leprae), *N. farcinica* (nocardiosis) and *Corynebacterium diphtheriae* (diphtheria) that exhibit a pronounced and broad natural resistance to various antimicrobial drugs and contribute towards various dangerous infections worldwide [22,23]. Hence, there is a strong interest in understanding the rate limiting steps of antibiotic transport through the channels. In this study, we focus on understanding the pathway of various hydrophilic antibiotics as well as solutes through the outer-membrane porin from the Gram-positive mycolata, *N. farcinica*.

The outer membrane porin from *N. farcinica* was first identified in 1998 [18], which was later resolved as a hetero-oligomeric channel composed of two different subunits; *NfpA* and *NfpB* [24]. The crystal structure of the protein is unknown but the sequence analysis suggests that it has a high homology to the MspA channel [24]. Previously, we have studied the translocation of polypeptides through the *N. farcinica* channel reconstituted into lipid bilayers [25]. In the present study, we focused on the functionality of the *N. farcinica* channel using planar lipid bilayer electrophysiology and liposome swelling assay. Liposome swelling assay was employed to study the translocation of various uncharged/zwitterionic hydrophilic nutrient molecules such as sugars and amino acids. Using single channel electrophysiology, we studied ion current fluctuations of the channel in the presence of clinically relevant antibiotic molecules; positively charged amikacin and kanamycin, and negatively charged ertapenem [18]. Additionally, we selectively neutralized the negatively charged amino acid residues at the pore

* Corresponding author at: Department of Chemistry, University of Oxford, Oxford OX1 3TA, United Kingdom. Tel.: +49 4212003588.
E-mail addresses: p.singh@jacobs-university.de (P.R. Singh), mahendran.kozhinjampararadhakrishnan@chem.ox.ac.uk (K.R. Mahendran).

http://dx.doi.org/10.1016/j.bbamem.2014.11.020
0005-2736/

lumen to elucidate the effect of charge on antibiotic–solute interaction within the channel.

2. Materials and methods

2.1. Bacterial strains and growth conditions

Escherichia coli cells containing the pARAJS2 vector with *NfpA* and *NfpB* genes were used in each experiment. For plasmid purification *E. coli* DH5Alpha cells were grown in LB medium at 37 °C with ampicillin antibiotic used for selection. *E. coli* BL21 (DE3) Omp8 was utilized for expression experiments. 100 μg/mL ampicillin and 40 μg/mL kanamycin were used for selection.

2.2. Site directed mutagenesis of genes NfpA and NfpB

Cultures of *E. coli* DH5Alpha grown at 37 °C, containing the pARAJS2 plasmids harboring wild-type (WT) genes, are used for extraction of the plasmid. *In vitro* site-directed mutagenesis was employed to obtain the desired mutations. The mutations were generated using two approaches; quick change site directed mutagenesis and the megaprimer method using PCR. The primers used to introduce substitution-mutations were listed in Supplementary Table 1. The PCR conditions used for quick change mutagenesis were: initial denaturing at 95 °C for 1 min, 30 cycles at 95 °C for 30 s, 55 °C for 1 min, 68 °C for 7 min and final extension at 68 °C for 10 min. Forward primer *NfpA* and reverse primer *NfpA* D141N D142N led to complete copy of pARAJS2 plasmid containing desired mutations. The megaprimer required two steps of PCR, first step led to megaprimers with typical lengths of 250–300 bp and in the second step these megaprimers were used as primers for second PCR. The conditions used were: first step 95 °C for 1 min, 30 cycles at 95 °C for 30 s, 55 °C for 1 min, 68 °C for 45 s and final extension at 68 °C for 5 min. The second step consisted of 95 °C for 10 min, 30 cycles at 95 °C for 1 min, 72 °C for 7 min and final extension at 72 °C for 30 min. *DpnI* digestion was carried out on the PCR product and then run on 1% agarose gel.

2.3. Protein expression and purification

The purification of the two subunits *NfpA* and *NfpB* expressed in *E. coli* BL21 (DE3) Omp8 was performed as described previously with slight modifications [24,25]. Briefly, pARAJS2_*nfpA* (mutant)/*nfpB* (mutant) transformed in the porin-deficient *E. coli* BL21(DE3)Omp8 cells was grown in LB media at 37 °C to an OD_{600} of 0.5–0.9. The cells were then induced with 0.02% of arabinose for over-expression of proteins and were grown at 16 °C for 16 h. The cells are collected by centrifugation at 5000 ×*g* for 20 min at 4 °C, and the resulting pellet was re-suspended in 10 mM Tris pH 8. The re-suspended pellet was broken down by French press, and the cell debris was separated by centrifugation at 5000 ×*g* for 10 min at 4 °C. The supernatant was ultra-centrifuged at 48,000 ×*g* for 1 h at 4 °C to separate the cytosolic proteins present in supernatant and the pellet containing membrane proteins. The protein of interest was further purified from the supernatant fraction to avoid contamination from membrane proteins of *E. coli* present in the pellet fraction. His-tagged protein purification from the supernatant fraction was then performed using Ni-NTA beads under denaturing conditions. The protein of interest was eluted using a gradient of imidazole concentration. The two subunits, purified separately, were refolded together to form a hetero-oligomeric channel by ammonium sulfate precipitation. The two purified subunits are mixed together in a 1:1 ratio and precipitated using saturated ammonium sulfate solution. The solution was incubated overnight at 4 °C and centrifuged at 18,000 ×*g* for 30 min. The precipitated protein pellet was refolded to native state by incubating at 4 °C in 150 mM NaCl, 25 mM Tris–HCl and 1% Genapol.

2.4. Liposome swelling assays

N. farcinica porin was reconstituted into liposomes as described by Nikaido and Rosenberg [26]. *E. coli* total lipid extract was used to form liposomes; 15% Dextran (MW 40,000) was used to entrap the liposomes, and their final size was checked using a Nano-ZS ZEN3600 zetasizer (Malvern Instruments, Malvern, United Kingdom). Control liposomes were prepared in the same manner but without the addition of porin. 0.5–1 μg of protein per 2 mg of lipid was used to make proteoliposomes. The concentrations of test solute were adjusted so that diluents were apparently isotonic with control liposomes. Stachyose was also tested with proteoliposomes to confirm the isotonicity of the multilamellar liposomes. Liposome or proteoliposome solution (30 μL) was diluted into 630 μL of an isotonic test/solute solution made in 10 mM Tris–HCl pH 7.5 buffer in a 1 mL cuvette and mixed manually. The change in absorbance at 500 nm was monitored using a Cary–Varian UV–vis spectrophotometer in the kinetic measurement mode. The swelling rates were taken as averages from at least five different sets of experiments, calculated as described previously [27].

2.5. Solvent free lipid bilayer technique

Reconstitution experiments and noise analysis have been performed as described in detail previously. The Montal and Muller technique was used to form phospholipid bilayer using DPhPC (Avanti polar lipids) [28]. A Teflon cell comprising an aperture of approximately 30–60 μm diameter was placed between the two chambers of the cuvette. The aperture was prepainted with 1% hexadecane in hexane for stable bilayer formation. 1 M KCl (or 150 mM KCl) and 10 mM HEPES, pH 7.4 were used as the electrolyte solution and added to both sides of the chamber. Ion current was detected using standard silver–silver chloride electrodes from WPI (World Precision Instruments) that were placed in each side of the cuvette. Single channel measurements were performed by adding the protein to the *cis*-side of the chamber (side connected to the ground electrode). Spontaneous channel insertion was typically obtained while stirring under applied voltage. Channel insertion was almost always oriented with the extracellular region facing *the cis-side*. After successful single channel reconstitution, the *cis*-side of the chamber was carefully perfused to remove any remaining porins to prevent further channel insertions. Conductance measurements were performed using an Axopatch 200B amplifier (Molecular devices) in the voltage clamp mode. Signals were filtered by an on board low pass Bessel filter at 10 kHz and with a sampling frequency set to 50 kHz. Amplitude, probability, and noise analyses were performed using Origin pro 8 (OriginLab) and Clampfit softwares (Molecular devices). Single channel analysis was used to determine the antibiotic binding kinetics. In a single-channel measurement the typical measured quantities were the duration of closed blocked levels' residence time (τ_c) and the frequency of blockage events (ν). The association rate constants k_{on} were derived using the number of blockage events, $k_{on} = \nu / [c]$, where c is the concentration of antibiotic. The dissociation rate constants (k_{off}) were determined by averaging the $1/\tau_c$ values recorded over the entire concentration range [29]. Similarly, the selectivity measurements were performed using two different salt solutions in the two chambers of the cuvette. The reverse potential required to obtain zero-current was calculated and the ratio of the permeabilities of cation/anion was calculated using the Goldman–Hodgkin–Katz equation [30,31].

3. Results and discussion

3.1. Mutational studies on N. farcinica cell wall channel

Based on the homology modeling of the porin with the known structure of MspA, we selected various negatively charged amino acids; located strategically at the periplasmic side of the channel in the two different subunits, *NfpA* and *NfpB*, and mutated them to neutral

amino acids with a similar length of the side chain. Table 1 shows the selected mutations in both subunits and the corresponding channel conductance of the mutant channels in 1 M KCl solution. In particular, we performed at maximum two mutations (D141N and D142N) in *NfpA* and 4 ones (E123Q, E144Q, D127N, E140Q) in *NfpB*, resulting in a total number of maximum 24 mutations in the pore-forming oligomer. Fig. 1 shows the expected positions of the mutations. Some other mutations led to proteins that had no channel-forming activity. This is presumably the result of the loss of channel function caused by the mutation of residues that were crucial for protein folding and assembly of the oligomers (Table 1). To elucidate the effect of charge residues inside the pore on the interaction with antibiotics, we choose the mutant oligomer with the highest number of negatively charged residues mutated to neutral ones and compared the effect of antibiotics on channel conductance with those on wild-type (WT) porin.

Based on homology modeling we created the surface potential of the porin and compared both the WT and the mutant channel as shown in Supplementary Fig. 1. The mutations rendered its periplasmic side rather neutral compared to the WT channel. To study the interaction of the mutant channel with cationic peptide we performed single-channel measurements to determine the approximate locations of these mutations. As shown in Supplementary Fig. 1A, we observed that hepta-arginine showed a very strong interaction with the WT channel resulting in frequent blockages of ionic current in multiple steps when added to the periplasmic side (*trans*) of the channel [25]. However, when the same experiment was performed with the mutant porins (Supplementary Fig. 1B), we observed reduced interactions of hepta-arginine with the channel. This reduction was due to the absence of negatively charged amino acids in the periplasmic entry of the pore, suggesting that the mutations were located at the correct positions.

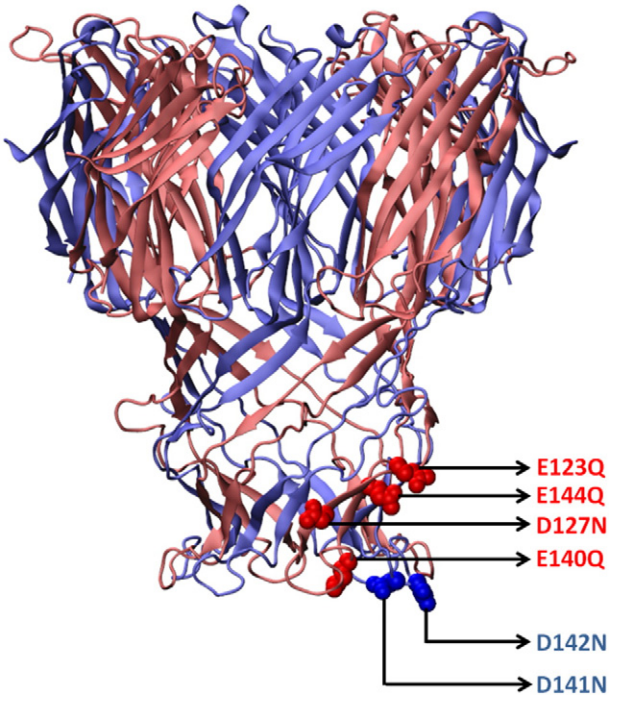

Fig. 1. Homology modeling of hetero-oligomeric *N. farcinica* channel based on the template MspA porin from *M. smegmatis* [25]. Selected mutations are shown for one *NfpA* monomer (blue) and one *NfpB* monomer (red) resulting in total of 24 mutations in the channel-forming oligomer. Note that the bottom side of the oligomer is exposed to the inner side of the mycolic acid layer and the top to the external medium. Reconstitution into lipid bilayer membranes occurs exclusively with the periplasmic side of the oligomer exposed to the *trans*-side of the bilayer.

3.2. Ion selectivity measurements

Ion selectivity measurements of both the WT and mutant pore were performed using different concentrations of monovalent KCl salt solutions on both sides of DphPC membranes. As expected, the channel was highly cation selective due to the large number of negatively charged residues inside the channel as shown in Table 2. As shown previously, the cation selectivity of the channel is not caused due to a particular binding site inside the channel but by the presence of point negative charges inside the lumen of the channel [18,32]. This changes the cation selectivity of the channel using different concentrations of the electrolyte solution on both sides of the membrane. At high salt concentration (1 M KCl/150 mM KCl), caused by electrostatic effects, the cation selectivity of the channel ($pK^+/pCl^- = 3.8$) was lower compared to the selectivity (7.8) at a lower salt concentration on both sides of the membranes (500 mM KCl/75 mM KCl). Similarly, the ion selectivity of the mutant pore was lower compared to WT pore in both salt concentrations, making it slightly less cation selective because many negatively charged groups became neutral by mutation.

3.3. Functional assays with liposomes

The channel functionality of *NfpA*/*NfpB* WT and mutant oligomers was further confirmed by reconstituting them in liposomes and measuring their permeability for small hydrophilic molecules such as sugars and amino acids. The rate of diffusion of sugars and amino acids was calculated by measuring the change in optical density of proteoliposomes in the presence of an isotonic concentration of sugars/amino acids [26]. Permeation rates were obtained within the same batch allowing us to normalize the diffusion rates with respect to arabinose [26]. We found that the exclusion limit of the channel was slightly higher than that observed in the case of Gram-negative porins, as shown in Fig. 2 by the considerably higher diffusion rate of large molecules, such as raffinose. This suggested a larger exclusion limit of the channel which may be due to the larger pore size of the channel. Importantly, these results were coherent with previous results for porin from *Mycobacterium chelonae* which has similar properties as the *N. farcinica* channel [14]. The highest diffusion rates were obtained for the two amino acids glycine and L-serine; they were approximately 80% higher than that observed for arabinose. The diffusion rates of other sugars including maltose, sucrose and glucose were approximately 20% lower than arabinose. Liposome swelling assays performed on *N. farcinica* channel indicated passive diffusion of different sugars and amino acids through the channel with the rate of permeation proportional to the size of the substrate. The diffusion rate was found to decrease with the increase of molecular mass of solutes as reported previously [14,26]. There was no significant difference in diffusion rates of sugar and amino acids between the WT and mutant protein. This was expected since all the

Table 1
Mutations performed in both the *NfpA* and *NfpB* subunits of *N. farcinica* porin. This table shows the conductance at 1 M KCl and 20 mM HEPES, pH 7.5 once the mutants have been refolded.

Mutations in *NfpA*	Mutations in *NfpB*	Average conductance (nS) n = 10
Wild-type (WT)	E123Q, E144Q, D127N, E140Q	3.1 ± 0.2
D141N, D142N	E123Q, D127N	2.8 ± 0.3
D141N, D142N	E123Q, E144Q, D127N, E140Q	2.7 ± 0.3 (selected for further studies)
D141N, D142N	E123Q, E144Q, D127R, E140Q	2.2 ± 0.1
E101K, D141N, D142N, D181R	E123Q, E144Q, D127N, E140Q	No channel-forming activity observed

Table 2
Ion selectivity of WT and mutant *N. farcinica* channels using different KCl concentration gradients on both sides of the DphPC membranes.

N. farcinica	Concentration gradient [*cis*/*trans*]	Reverse potential on the more dilute side [mV]	Pc/Pa (n = 3)
Wild-type (WT)	1 M KCl/150 mM KCl	23 ± 1	3.8 ± 0.2
	500 mM KCl/75 mM KCl	33 ± 1	7.8 ± 0.3
Mutant	1 M KCl/150 mM KCl	21 ± 1	3.2 ± 0.2
NfpA (D141N, D142N)	500 mM KCl/75 mM KCl	27 ± 1	4.8 ± 0.2
NfpB (E123Q, E144Q, D127N, E140Q)			

sugars or amino acids tested were neutral or zwitterionic. Furthermore, we also performed single channel electrophysiology experiment on sugar transport through the *N. farcinica* channel. However, it seemed that the sugar molecules did probably not bind inside the channel. They diffused through the channel which means that our instrumental set-up could not resolve any interaction between sugars and channel in terms of ion current fluctuations.

3.4. Interaction between antibiotics and the N. farcinica channel

One of the main focuses in this study was to investigate the interaction of clinically relevant antibiotics with the *N. farcinica* channel. Identifying the antibiotic affinity site and its position inside the channel helps to understand the rate limiting interaction and sheds light on the pathway of the antibiotic through the channel [33–36]. Based on the selectivity of the *N. farcinica* channel and the presence of negatively charged residues in the channel's mouth, it has been postulated that positively charged antibiotic may utilize this channel as the pathway for permeation [18]. Using this assumption, we selected two positively charged aminoglycosides for our study, kanamycin and amikacin.

The *N. farcinica* channel has a strong asymmetry of the channel gating such that it is highly stable at negative voltages but gates significantly at positive voltages as low as +30 mV (protein addition to the *cis*/ground side) [25]. Thus the majority of the experiments were performed at negative voltages at the *trans*-side. In the absence of antibiotics, no fluctuation in the ion current was detected here and in a previous study [18,25]. This changed completely when amikacin and kanamycin were added in μM concentration to the *cis*-side of the membranes. Ion current fluctuations observed for both amikacin and kanamycin at 150 mM KCl solution are shown in Figs. 3A and 4A, respectively. Addition of antibiotics to the *cis* (ground) side of the channel induced ion current blocks, suggesting possible antibiotic–porin interaction. In contrast to this, we did not observe at applied positive voltages any interactions, which might be caused by the positive voltage repelling the positively charged antibiotic molecules from the channel. As a control we reversed the experiment with respect to voltage. Addition of the antibiotics to the *trans*-side under negative voltages also caused no ion current fluctuations.

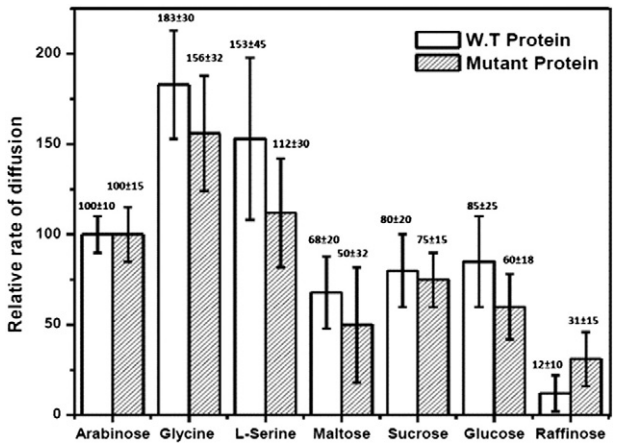

Fig. 2. Liposome swelling assay performed for both WT and mutant *N. farcinica* porins reveals the qualitative diffusion rate of different sugars and amino acids based on their sizes. Note that the difference of the relative rate of diffusion between the WT channel and its mutant was within the SD of the experimental error.

The most prominent interactions were observed at *cis* addition and applied negative voltages with a lowered salt solution from 1 M KCl to 150 mM KCl. This suggested that the interaction between the antibiotic and porin had a strong charge–charge interaction component. Similarly, previous experiments that have been performed on peptides and DNA molecules have also reported this enhanced interaction, upon lowering of the salt concentration [37,38].

Amikacin is an aminoglycoside with a net positive charge of 4 at pH 7.4 [39]. Increasing the concentration of amikacin showed increased interaction with both the WT and mutant channels. However, addition of amikacin to the mutant pore with <24 negative amino acid residues showed significantly less interaction than the WT channel, as depicted by the ion current trace in Fig. 3D. The current amplitude histogram shown in Fig. 3B and E provides the decreased current counts of the closed state (blocked state) in the mutant pore compared to those of WT. The scatter plot of amplitude (y-axis) and dwell time (x-axis), Fig. 3C and F, represents the antibiotic–channel interactions. The residence (dwell) time of antibiotic interaction with the porin ranged from 100 μs to 800 μs with an average residence time of 200 μs for the WT channel. In the case of the mutant channel, the average residence time decreased to something like 100 μs close to the time resolution limit of our instrumentation. We also observe a slight decrease in amplitude of amikacin blocking in mutant channel compared to the WT channel, which is due to the decrease in the overall conductance of the mutant channel (Table 1).

Similarly, kanamycin is also an aminoglycoside with a net positive charge of 4 and as expected, kanamycin also showed interaction with the pore. Nevertheless, the interaction of kanamycin was significantly different to that observed for amikacin (Figs. 3A and 4A). Kanamycin exhibited lower frequency of events compared to amikacin. In addition, the interaction of kanamycin with the pore was not uniform as depicted in the plots in Fig. 4B and E. From Fig. 4C, we observed that the dwell times of the kanamycin interaction ranged from 100 μs to 80 ms. This suggested that kanamycin may have more than one binding site within the channel surface. Likewise to amikacin, the number of events and the residence time of kanamycin interaction decreased in the mutant pore as shown in Fig. 4D and F.

Previous reports on antibiotic translocations through porins of Gram-negative bacteria highlight that charged residues within a pore influence the interaction between the antibiotics and pore and hence the rate of translocation [40–45]. Mutation of amino acid D113N of *E. coli* OmpF loop 3 shows an increased rate of permeation of ampicillin [42]. Similarly, a single mutation in the loop 3 region (glycine to aspartate) of *Enterobacter aerogenes* Omp36 porin exhibits a reduced pore conductance and decreased cephalosporin permeation [46]. To elucidate the importance of charge and the presence of affinity site inside the porin, we performed an antibiotic titration experiment with *N. farcinica* mutant pore, where 24 amino-acids were neutralized. In such an experiment (Supplementary Table 2), we observed that both

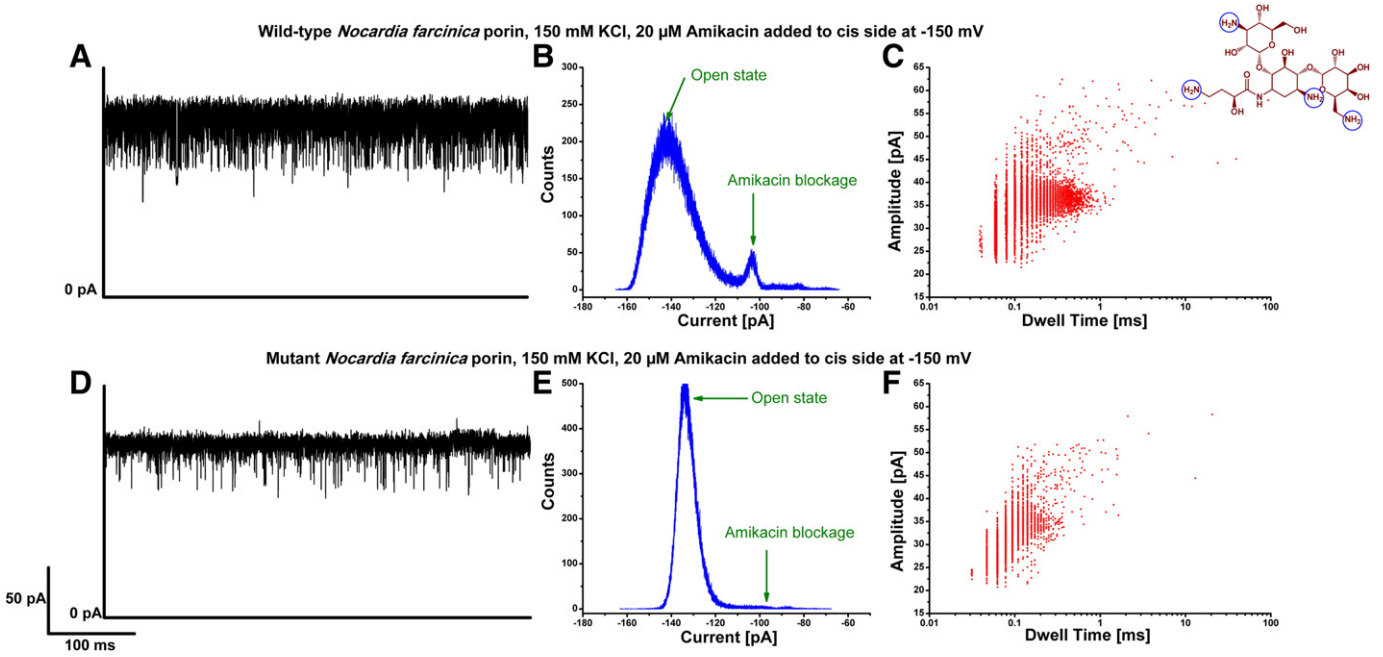

Fig. 3. Interaction of amikacin (chemical structure top right) with WT and mutant *N. farcinica* channel. (A) 20 μM amikacin was added to the *cis*-side of the WT channel at an applied voltage of −150 mV. (B) Event histogram of amikacin with the WT channel. (C) Amplitude-dwell time scatter plot of amikacin events with the WT channel. (D) 20 μM amikacin was added to the *cis*-side of the mutant channel at an applied voltage of −150 mV. (E) Event histogram of amikacin with the mutant channel. (F) Amplitude-dwell time scatter plot of amikacin events with the mutant channel. Experimental conditions were 150 mM KCl and 10 mM HEPES, pH 7.4.

the on-rate as well as the residence time of amikacin and kanamycin were reduced for the mutated pore, emphasizing the importance of affinity sites inside the channel.

In our experiment, both the positively charged antibiotics belong to the antibiotic class of aminoglycoside. Amikacin and kanamycin both possess 4 positive charges at pH 7.4 and the structures of the antibiotics share a similar scaffold. However, we observed a very sharp difference in the binding kinetics of these two antibiotics with the pore. Amikacin had a significantly higher on-rate as compared to kanamycin (Supplementary Table 2). *In vivo* Minimum Inhibitory Concentration (MIC) assay of different antibiotics performed with *N. farcinica* showed amikacin to be an effective drug compared to kanamycin [47,48]. Could the higher on-rate of amikacin compared to kanamycin be the reason for such difference in effectiveness? However, the presented

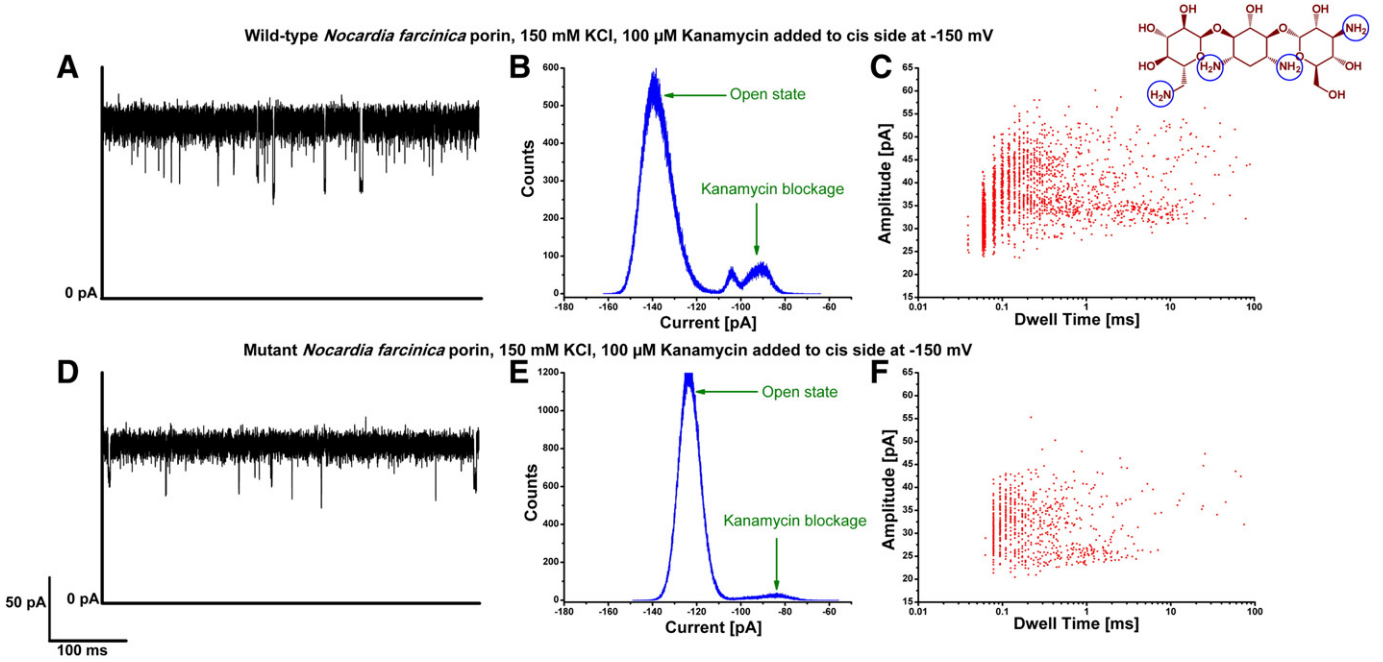

Fig. 4. Interaction of kanamycin (chemical structure top right) with WT and mutant *N. farcinica* channel. (A) 100 μM kanamycin was added to the *cis*-side of the WT channel at an applied voltage of −150 mV. (B) Event histogram of kanamycin with the WT channel. (C) Amplitude-dwell time scatter plot of kanamycin events with the WT channel. (D) 100 μM kanamycin was added to the *cis*-side of the mutant channel at an applied voltage of −150 mV. (E) Event histogram of kanamycin with the mutant channel. (F) Amplitude-dwell time scatter plot of kanamycin events with the mutant channel. Experimental conditions were 150 mM KCl and 10 mM HEPES, pH 7.4.

results of channel blocking cannot be converted directly into translocation, since binding does not always imply translocation. For uncharged solutes, liposome swelling assays can be performed to distinguish if the molecule is indeed permeating through the channel, which is not feasible with charged molecules. For charged molecules, as in our case; we performed a voltage dependent analysis of kinetic off-rate to distinguish binding from translocation as previously reported to distinguish binding from translocation for short peptides [25,49].

Increasing voltages tended to increase the residence time of the kanamycin, whereas the residence time of amikacin decreased as shown in Fig. 5. As mentioned earlier, the average residence time of amikacin was 200 μs at −150 mV. An increase of the external voltage up to −200 mV resulted in an overall decrease of the channel conductance instead of observing single ion fluctuation events. This may be due to significantly fast permeation events. However, in the case of kanamycin, increasing the voltage increased the residence time of the antibiotic. At high voltages (>200 mV), we observed an apparent strong binding which suggested that the molecule is held inside the pore in such a way that the pore remained in its closed state (figure not shown). The abovementioned observation suggested that amikacin is permeating through the channel; whereas kanamycin is not able to penetrate the channel, supporting the susceptibility of *N. farcinica* for amikacin over kanamycin. The impermeability of kanamycin through the homologous MspA porin using MIC assays has also been reported earlier, which correlated with our results [20,50]. However, *in vivo* biological systems can be far more complicated and there could be other probable reasons for such discrepancy in susceptibility. Even though we cannot directly compare the *in vitro* results obtained using single channel electrophysiology to the *in vivo* data, here we present an important factor of antibiotic permeability (by distinguishing binding and translocation) through the porins that could alter the effectiveness of antibiotics.

Apart from the positively charged antibiotics, we also investigated various chemically and structurally/clinically relevant antibiotics such as fluoroquinolones, penicillins, carbapenems and sulfonamides [47,48,51]. Most of these antibiotics are either zwitterionic or negatively charged and thus no interaction was observed with the highly negatively charged amino acids inside the pore lumen of the *N. farcinica* porin. Surprisingly, addition of the carbapenem antibiotic ertapenem showed ion current fluctuation with the single *N. farcinica* channel (Fig. 6A). Ertapenem, which is a negatively charged antibiotic, is prone to repulsive forces from the negatively charged interior of the channel. This implies that the interaction observed with the antibiotic and the pore could be due to non-ionic interactions. To confirm the role of electrostatic interaction between antibiotic and pore, we performed our experiments in both 1 M and 150 mM KCl solution and found that the interaction was similar (*i.e.* residence time of ertapenem inside the pore was ~200 μs) in both cases, supporting the assumption of non-ionic interaction (Supplementary Fig. 2). By looking at the structure of ertapenem, we noted that it consists of multiple aromatic rings; which, as we hypothesize, may interact with the hydrophobic amino acids inside the pore lumen.

Ion current blockages were observed for both the WT and mutant porins in the presence of ertapenem and an increased number of events were observed with increased ertapenem concentration as shown in Fig. 6C. The event frequency of ertapenem was similar in both WT and mutant when the antibiotic was added to the *cis* (extracellular) side; however a significant difference was observed for the event frequency when the antibiotic was added to the *trans* (periplasmic) side as shown in Fig. 6A and B. The mutant pore exhibited a higher number of ertapenem interactions in comparison to WT pore. During the entry of ertapenem into the channel from the periplasmic side, it faces strong repulsive forces from the surrounding negatively charged amino acids. In contrast, when the negatively charged residues in the periplasmic space were neutralized, the lower repulsive forces in this case seemed to enhance the on-rate of ertapenem with the channel. Previous reports on MspA porin from *M. smegmatis* that has point negative charges in the mouth of the channel reported a 10-fold lower permeability of monoanionic beta-lactams compared to zwitterionic cephaloridine [52]. The presence of a negatively charged residue in the mouth of the channel affected the permeation of a negatively charged molecule, which correlates well with our observations.

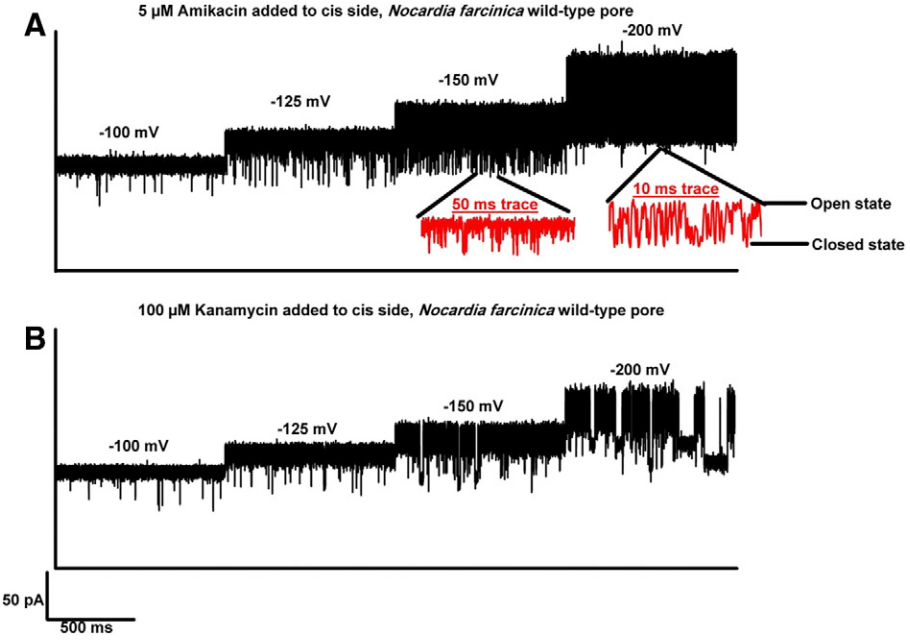

Fig. 5. Distinguishing binding from translocation: Voltage scan of ion current fluctuation of antibiotics through the *N. farcinica* channel. (A) Increasing the application of external voltage with addition of amikacin to the *cis*-side of the channel. At higher voltages, the residence time of the channel decreased to the limit of the instrument and could not be resolved. (B) Increasing the application of external voltage with addition of kanamycin to the *cis*-side of the channel. With increasing voltage, the binding of kanamycin with the channel increases. Experimental conditions were 150 mM KCl and 10 mM HEPES, pH 7.4.

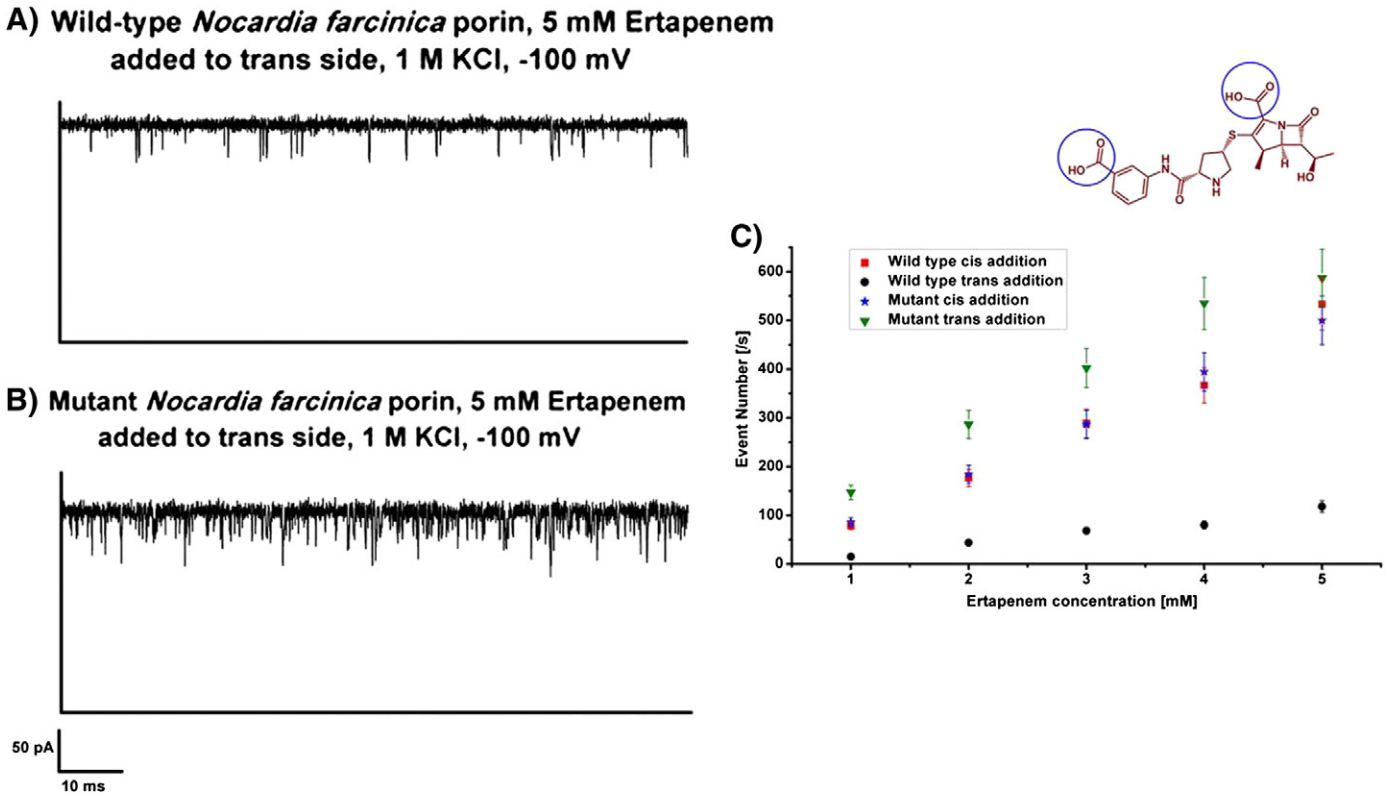

Fig. 6. Interaction of ertapenem (chemical structure top right) with WT and mutant *N. farcinica* channel. Ion current trace obtained when ertapenem was added to the *trans*-side of the channel at an applied voltage of −100 mV for (A) WT porin and (B) mutant porin. (C) Number of event plotted against concentration of ertapenem added to both WT and mutant porin in both extracellular (*cis*) and periplasmic (*trans*) side of the channel. Experimental conditions were 1 M KCl and 10 mM HEPES, pH 7.4.

4. Conclusion

Mycolata have evolved a complex cell wall, comprising peptidoglycan–arabinogalactan polymer covalently bound to mycolic acids of considerable size (up to 90 carbon atoms), a variety of extractable lipids, and pore-forming proteins [11,53,54]. Since the role of the outer-membrane is indispensable in the mycobacterial resistance to antibiotics, it is tempting to reconstitute the porins in a mycolic acid containing bilayer to retain their physiological environment. Reconstitution of MspA from *M. smegmatis* in mycolic acid membrane has been studied before [55], however, our effort to form and reconstitute the *N. farcinica* porin in the mycolic acid containing membrane was unsuccessful. Nonetheless, we were able to successfully reconstitute the protein in phospholipid bilayers and liposomes to perform single channel measurements and liposome swelling assays.

Current investigation represents one of the first detailed studies on solute and antibiotic permeation through porin from bacterium belonging to mycolata. We have confirmed the channel functionality of *N. farcinica* porin using liposome swelling assays and permeation of nutrient molecules including different sized sugars and amino acids. In addition to different solutes, the interaction of clinically relevant antibiotics such as amikacin, kanamycin and ertapenem was also studied at the single molecule level. Well defined ion current fluctuations were observed in the presence of these antibiotics that interact with the pore. We were also able to distinguish between translocation and binding for amikacin and kanamycin using voltage dependent analysis. Our results indicated that kanamycin was unable to translocate while amikacin was able to translocate through the channel. Furthermore, we elucidated the effect of various charged amino acids present inside the channel on the permeation of charged antibiotics and uncharged/zwitterionic molecules.

Acknowledgement

We would like to thank Dr. Niraj Modi for discussions and modeling of the *N. farcinica* channel and the Deutsche Forschungsgemeinschaft (DFG) through Wi2278/18-1 for financial support.

Appendix A. Supplementary data

Supplementary data to this article can be found online at http://dx.doi.org/10.1016/j.bbamem.2014.11.020.

References

[1] H. Nikaido, Prevention of drug access to bacterial targets: permeability barriers and active efflux, Science 264 (1994) 382–388, http://dx.doi.org/10.1126/science.8153625.
[2] H. Nikaido, Molecular basis of bacterial outer membrane permeability revisited, Microbiol. Mol. Biol. Rev. 67 (2003) 593–656.
[3] A.H. Delcour, Outer membrane permeability and antibiotic resistance, Biochim. Biophys. Acta 1794 (2009) 808–816, http://dx.doi.org/10.1016/j.bbapap.2008.11.005.
[4] J.-M. Pagès, C.E. James, M. Winterhalter, The porin and the permeating antibiotic: a selective diffusion barrier in Gram-negative bacteria, Nat. Rev. Microbiol. 6 (2008) 893–903, http://dx.doi.org/10.1038/nrmicro1994.
[5] K. Poole, Outer membranes and efflux: the path to multidrug resistance in Gram-negative bacteria, Curr. Pharm. Biotechnol. 3 (2002) 77–98.
[6] H. Nikaido, Outer membrane barrier as a mechanism of antimicrobial resistance, Antimicrob. Agents Chemother. 33 (1989) 1831–1836, http://dx.doi.org/10.1128/AAC.33.11.1831.
[7] T.J. Silhavy, D. Kahne, S. Walker, The bacterial cell envelope, Cold Spring Harb. Perspect. Biol. 2 (2010) a000414, http://dx.doi.org/10.1101/cshperspect.a000414.
[8] V. Jarlier, H. Nikaido, Mycobacterial cell wall: structure and role in natural resistance to antibiotics, FEMS Microbiol. Lett. 123 (1994) 11–18.
[9] V. Jarlier, L. Gutmann, H. Nikaido, Interplay of cell wall barrier and beta-lactamase activity determines high resistance to beta-lactam antibiotics in *Mycobacterium chelonae*, Antimicrob. Agents Chemother. 35 (1991) 1937–1939, http://dx.doi.org/10.1128/AAC.35.9.1937.

[10] D.E. Minnikin, S.M. Minnikin, M. Goodfellow, J.L. Stanford, The mycolic acids of *Mycobacterium chelonei*, J. Gen. Microbiol. 128 (1982) 817–822, http://dx.doi.org/10.1099/00221287-131-9-2237.

[11] D.E. Minnikin, Chemical principles in the organization of lipid components in the mycobacterial cell envelope, Res. Microbiol. 142 (1991) 423–427, http://dx.doi.org/10.1016/0923-2508(91)90114-P.

[12] P.J. Brennan, H. Nikaido, The envelope of mycobacteria, Annu. Rev. Biochem. 64 (1995) 29–63, http://dx.doi.org/10.1146/annurev.biochem.64.1.29.

[13] D.E. Minnikin, S.M. Minnikin, J.H. Parlett, M. Goodfellow, M. Magnusson, Mycolic acid patterns of some species of *Mycobacterium*, Arch. Microbiol. 139 (1984) 225–231, http://dx.doi.org/10.1007/BF00402005.

[14] J. Trias, V. Jarlier, R. Benz, Porins in the cell wall of mycobacteria, Science 258 (1992) 1479–1481, http://dx.doi.org/10.1126/science.1279810.

[15] M. Niederweis, Mycobacterial porins — new channel proteins in unique outer membranes, Mol. Microbiol. 49 (2003) 1167–1177, http://dx.doi.org/10.1046/j.1365-2958.2003.03662.x.

[16] T. Lichtinger, A. Burkovski, M. Niederweis, R. Krámer, R. Benz, Biochemical and biophysical characterization of the cell wall porin of *Corynebacterium glutamicum*: the channel is formed by a low molecular mass polypeptide, Biochemistry 37 (1998) 15024–15032, http://dx.doi.org/10.1021/bi980961e.

[17] J. Trias, R. Benz, Permeability of the cell wall of *Mycobacterium smegmatis*, Mol. Microbiol. 14 (1994) 283–290, http://dx.doi.org/10.1111/j.1365-2958.1994.tb01289.x.

[18] F.G. Riess, T. Lichtinger, R. Cseh, A.F. Yassin, K.P. Schaal, R. Benz, The cell wall porin of *Nocardia farcinica*: biochemical identification of the channel-forming protein and biophysical characterization of the channel properties, Mol. Microbiol. 29 (1998) 139–150, http://dx.doi.org/10.1046/j.1365-2958.1998.00914.x.

[19] C.M. Jones, M. Niederweis, Role of porins in iron uptake by *Mycobacterium smegmatis*, J. Bacteriol. 192 (2010) 6411–6417.

[20] O. Danilchanka, M. Pavlenok, M. Niederweis, Role of porins for uptake of antibiotics by *Mycobacterium smegmatis*, Antimicrob. Agents Chemother. 52 (2008) 3127–3134, http://dx.doi.org/10.1128/AAC. 00239-08.

[21] R. Benz, Bacterial Cell Wall, Elsevier, 1994., http://dx.doi.org/10.1016/S0167-7306(08)60422-6.

[22] World Health Organization, Global Tuberculosis Control 2011, , 2011, ISBN 978 92 9061 522 4.

[23] B.R. Bloom, Vaccines for the Third World, Nature 342 (1989) 115–120.

[24] C. Kläckta, P. Knörzer, F. Riess, R. Benz, Hetero-oligomeric cell wall channels (porins) of *Nocardia farcinica*, Biochim. Biophys. Acta Biomembr. 1808 (2011) 1601–1610, http://dx.doi.org/10.1016/j.bbamem.2010.11.011.

[25] P.R. Singh, I. Bárcena-Uribarri, N. Modi, U. Kleinekathöfer, R. Benz, M. Winterhalter, et al., Pulling peptides across nanochannels: resolving peptide binding and translocation through the hetero-oligomeric channel from *Nocardia farcinica*, ACS Nano 6 (2012) 10699–10707, http://dx.doi.org/10.1021/nn303900y.

[26] H. Nikaido, E.Y. Rosenberg, Porin channels in *Escherichia coli*: studies with liposomes reconstituted from purified proteins, J. Bacteriol. 153 (1983) 241–252.

[27] F. Yoshimura, H. Nikaido, Diffusion of beta-lactam antibiotics through the porin channels of *Escherichia coli* K-12, Antimicrob. Agents Chemother. 27 (1985) 84–92.

[28] M. Montal, P. Mueller, Formation of bimolecular membranes from lipid monolayers and a study of their electrical properties, Proc. Natl. Acad. Sci. U. S. A. 69 (1972) 3561–3566, http://dx.doi.org/10.1073/pnas.69.12.3561.

[29] E.M. Nestorovich, C. Danelon, M. Winterhalter, S.M. Bezrukov, Designed to penetrate: time-resolved interaction of single antibiotic molecules with bacterial pores, Proc. Natl. Acad. Sci. U. S. A. 99 (2002) 9789–9794, http://dx.doi.org/10.1073/pnas.152206799.

[30] A.L. Hodgkin, B. Katz, The effect of sodium ions on the electrical activity of the giant axon of the squid, J. Physiol. 108 (1949) 37–77.

[31] C. Danelon, A. Suenaga, M. Winterhalter, I. Yamato, Molecular origin of the cation selectivity in OmpF porin: single channel conductances vs. free energy calculation, Biophys. Chem. 104 (2003) 591–603, http://dx.doi.org/10.1016/S0301-4622(03)00062-0.

[32] J. Trias, R. Benz, Characterization of the channel formed by the mycobacterial porin in lipid bilayer membranes. Demonstration of voltage gating and of negative point charges at the channel mouth, J. Biol. Chem. 268 (1993) 6234–6240.

[33] H. Bajaj, Q.T. Tran, K.R. Mahendran, C. Nasrallah, J.P. Colletier, A. Davin-Regli, et al., Antibiotic uptake through membrane channels: role of *Providencia stuartii* ompPst1 porin in carbapenem resistance, Biochemistry 51 (2012) 10244–10249, http://dx.doi.org/10.1021/bi301398j.

[34] K.R. Mahendran, M. Kreir, H. Weingart, N. Fertig, M. Winterhalter, Permeation of antibiotics through *Escherichia coli* OmpF and OmpC porins: screening for influx on a single-molecule level, J. Biomol. Screen. 15 (2010) 302–307, http://dx.doi.org/10.1177/1087057109357791.

[35] B.K. Ziervogel, B. Roux, The binding of antibiotics in OmpF porin, Structure 21 (2013) 76–87, http://dx.doi.org/10.1016/j.str.2012.10.014.

[36] P.R. Singh, M. Ceccarelli, M. Lovelle, M. Winterhalter, K.R. Mahendran, Antibiotic permeation across the OmpF channel: modulation of the affinity site in the presence of magnesium, J. Phys. Chem. B 116 (2012) 4433–4438, http://dx.doi.org/10.1021/jp2123136.

[37] D. Fologea, J. Uplinger, B. Thomas, D.S. McNabb, J. Li, Slowing DNA translocation in a solid-state nanopore, Nano Lett. 5 (2005) 1734–1737, http://dx.doi.org/10.1021/nl051063o.

[38] K.R. Mahendran, M. Romero-Ruiz, A. Schlösinger, M. Winterhalter, S. Nussberger, Protein translocation through Tom40: kinetics of peptide release, Biophys. J. 102 (2012) 39–47, http://dx.doi.org/10.1016/j.bpj.2011.11.4003.

[39] R.S. Kane, P.T. Glink, R.G. Chapman, J.C. McDonald, P.K. Jensen, H. Gao, et al., Basicity of the amino groups of the aminoglycoside amikacin using capillary electrophoresis and coupled CE–MS–MS techniques, Anal. Chem. 73 (2001) 4028–4036, http://dx.doi.org/10.1021/ac010173m.

[40] C. Danelon, E.M. Nestorovich, M. Winterhalter, M. Ceccarelli, S.M. Bezrukov, Interaction of zwitterionic penicillins with the OmpF channel facilitates their translocation, Biophys. J. 90 (2006) 1617–1627, http://dx.doi.org/10.1529/biophysj.105.075192.

[41] K.R. Mahendran, E. Hajjar, T. MacH, M. Lovelle, A. Kumar, I. Sousa, et al., Molecular basis of enrofloxacin translocation through OmpF, an outer membrane channel of *Escherichia coli* — when binding does not imply translocation, J. Phys. Chem. B 114 (2010) 5170–5179, http://dx.doi.org/10.1021/jp911485k.

[42] E. Hajjar, K.R. Mahendran, A. Kumar, A. Bessonov, M. Petrescu, H. Weingart, et al., Bridging timescales and length scales: from macroscopic flux to the molecular mechanism of antibiotic diffusion through porins, Biophys. J. 98 (2010) 569–575, http://dx.doi.org/10.1016/j.bpj.2009.10.045.

[43] S. Vidal, J. Bredin, J.M. Pagès, J. Barbe, β-Lactam screening by specific residues of the OmpF eyelet, J. Med. Chem. 48 (2005) 1395–1400, http://dx.doi.org/10.1021/jm049652e.

[44] S.A. Benson, J.L. Occi, B.A. Sampson, Mutations that alter the pore function of the OmpF porin of *Escherichia coli* K12, J. Mol. Biol. 203 (1988) 961–970, http://dx.doi.org/10.1016/0022-2836(88)90121-0.

[45] R. Misra, S.A. Benson, Isolation and characterization of OmpC porin mutants with altered pore properties, J. Bacteriol. 170 (1988) 528–533.

[46] A. Thiolas, C. Bornet, A. Davin-Régli, J.M. Pagès, C. Bollet, Resistance to imipenem, cefepime, and cefpirome associated with mutation in Omp36 osmoporin of *Enterobacter aerogenes*, Biochem. Biophys. Res. Commun. 317 (2004) 851–856, http://dx.doi.org/10.1016/j.bbrc.2004.03.130.

[47] J. Ishikawa, A. Yamashita, Y. Mikami, Y. Hoshino, H. Kurita, K. Hotta, et al., The complete genomic sequence of *Nocardia farcinica* IFM 10152, Proc. Natl. Acad. Sci. U. S. A. 101 (2004) 14925–14930, http://dx.doi.org/10.1073/pnas.0406410101.

[48] E. Cercenado, M. Marín, M. Sánchez-Martínez, O. Cuevas, J. Martínez-Alarcón, E. Bouza, In vitro activities of tigecycline and eight other antimicrobials against different *Nocardia* species identified by molecular methods, Antimicrob. Agents Chemother. 51 (2007) 1102–1104, http://dx.doi.org/10.1128/AAC. 01102-06.

[49] L. Movileanu, J.P. Schmittschmitt, J.M. Scholtz, H. Bayley, Interactions of peptides with a protein pore, Biophys. J. 89 (2005) 1030–1045, http://dx.doi.org/10.1529/biophysj.104.057406.

[50] J. Stephan, C. Mailaender, G. Etienne, M. Daffé, M. Niederweis, Multidrug resistance of a porin deletion mutant of *Mycobacterium smegmatis*, Antimicrob. Agents Chemother. 48 (2004) 4163–4170, http://dx.doi.org/10.1128/AAC. 48.11.4163-4170.2004.

[51] O.H. Torres, P. Domingo, R. Pericas, P. Boiron, J.A. Montiel, G. Vázquez, Infection Caused by *Nocardia farcinica*: Case Report and Review, 2000., http://dx.doi.org/10.1007/s100960050460.

[52] V. Jarlier, H. Nikaido, Permeability barrier to hydrophilic solutes in *Mycobacterium chelonei*, J. Bacteriol. 172 (1990) 1418–1423.

[53] H. Gebhardt, X. Meniche, M. Tropis, R. Krämer, M. Daffé, S. Morbach, The key role of the mycolic acid content in the functionality of the cell wall permeability barrier in *Corynebacterineae*, Microbiology 153 (2007) 1424–1434, http://dx.doi.org/10.1099/mic. 0.2006/003541-0.

[54] C.E. Barry, R.E. Lee, K. Mdluli, A.E. Sampson, B.G. Schroeder, R.A. Slayden, et al., Mycolic acids: structure, biosynthesis and physiological functions, Prog. Lipid Res. 37 (1998) 143–179, http://dx.doi.org/10.1016/S0163-7827(98)00008-3.

[55] K.W. Langford, B. Penkov, I.M. Derrington, J.H. Gundlach, Unsupported planar lipid membranes formed from mycolic acids of *Mycobacterium tuberculosis*, J. Lipid Res. 52 (2011) 272–277, http://dx.doi.org/10.1194/jlr.M012013.